Glass-Encapsulated Light Harvesters: More Efficient Dye-Sensitized Solar Cells by Deposition of Self-Aligned, Conformal, and Self-Limited Silica Layers

Glass-Encapsulated Light Harvesters: More Efficient Dye-Sensitized Solar Cells by Deposition of Self-aligned, Conformal and Self-limited Silica Layers

Ho-Jin Son,[†,||] Xinwei Wang,[‡,||] Chaiya Prasittichai,[†] Nak Cheon Jeong,[†] Titta Aaltonen,[‡,+] Roy G. Gordon,[‡,*] Joseph T. Hupp[†,§,*]

[†]*Department of Chemistry and Argonne-Northwestern Solar Energy Research (ANSER) Center, Northwestern University, Evanston, IL 60208, United States*

[‡]*Department of Chemistry and Chemical Biology, Harvard University, Cambridge, Massachusetts 02138, United States*

[§]*Argonne National Laboratory, 9700 South Cass Ave., Argonne, IL 60439, United States*

Supporting Information Placeholder

ABSTRACT: A major loss mechanism in dye-sensitized solar cells (DSCs) is recombination at the TiO_2/electrolyte interface. Here we report a method to reduce greatly this loss mechanism. We deposit insulating and transparent silica (SiO_2) onto the open areas of a nanoparticulate TiO_2 surface while avoiding any deposition of SiO_2 over or under the organic dye molecules. The silica coating covers the highly convoluted surface of the TiO_2 conformally and with a uniform thickness throughout the thousands of layers of nanoparticles. DSCs incorporating these selective and self-aligned SiO_2 layers achieved a 36% increase in relative efficiency versus control uncoated cells.

Dye-sensitized solar cells (DSCs) have great potential to compete with conventional p–n junction solar cells due to their relatively low-cost.[1] However, their efficiency is limited by the ease with which electrons collected by the nanoparticle framework can recombine with ions in solution. Therefore, the photovoltaic efficiency of DSCs can be increased by retarding electron recombination at the photoelectrode interfaces. The surfaces of the TiO_2 nanoparticles are not fully covered by the dye molecules as shown schematically in Figure 1. Thus an electrical short by direct contact between electrolyte and the areas of TiO_2 not covered by dye provides an important loss pathway by which electrons recombine with the electrolyte. This recombination rate could be reduced or eliminated by selectively coating an insulating and transparent layer on these open areas of TiO_2. In an effort to minimize such losses, many groups have proposed device architectures that include the coating of inorganic barrier layers,[2] the use of long aliphatic chain on organic framework,[3] saccharides,[4] the introduction of co-adsorbents,[5] encapsulation by cyclodextrins (CDs),[6] and post-surface passivation by polymerization.[7] Recently high band gap metal oxide layers prepared via atomic layer deposition (ALD) have received much attention as an efficient interface engineering tool owing to its capability of infiltrating porous structures thereby ensuring good coverage of the surface of the nanoporous electrode,[8] fine control of thickness,[9] and low temperature processing.[10] However, applying ALD layers prior to dye adsorption on TiO_2 or related oxides significantly reduces the electron transfer rate from the dye through the metal oxide over-layers by creating a tunneling barrier.[11] Therefore, a new methodology is needed that does not interfere with electron transfer to or from the dye molecules.

Scheme 1. Schematic diagram depicting post-dye SiO_2 deposition process and plausible reaction mechanism on dye-coated TiO_2 nanoparticles

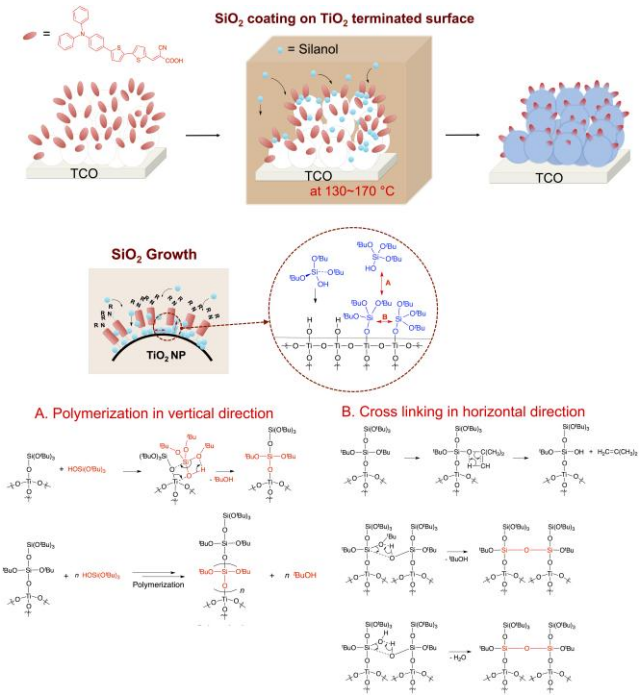

We discovered a method to deposit selectively an insulating and transparent layer of silica (SiO_2) only on the open areas of TiO_2 surface, but not on the adsorbed dye molecules or between the dye surface-linker and the electrode. Our approach exploits deposition of SiO_2 from a precursor that is catalytically decomposed by the surface of TiO_2. Areas of TiO_2 covered by adsorbed dye do not catalyze the deposition of SiO_2. Thus the gaps between dye molecules are selectively covered by SiO_2. This SiO_2 retards the interfacial charge recombination dynamics without hindering electron injection from the dye into the TiO_2 or from the solution into the dye. When this SiO_2 treatment was applied to a DSC just after coating the TiO_2

with an organic dye (**OrgD**, Scheme 1), enhanced performance was obtained, with a higher power conversion efficiency and longer electron lifetime. Another important feature of the SiO_2 deposition process is that its thickness is self-limiting, so the same thickness is applied to all levels in the porous multilayer structure of the photo-electrode. In this study, we investigated the conditions needed to make SiO_2 deposit selectively on TiO_2 between dyes.

We found that silica less than 1 nanometer thick functions as a barrier to charge recombination and thereby improves the performance of these photovoltaic devices. The SiO_2 coating chemistry is related to a process for rapid atomic layer deposition (ALD) using alternating exposure of surfaces to vapors of trimethylaluminum (TMA) as a catalyst and tris(*tert*-butoxy)silanol (TBOS) as the SiO_2 precursor.[12] In this reaction, aluminum placed on the surface by the TMA plays a crucial role as a Lewis-acidic catalyst for deposition of silica layers up to 15 nm thick on top of the alumina.[13] There have been reports that hafnium and zirconium can also catalyze the growth of SiO_2.[14-16] This work suggested to us that titanium might also catalyze the growth of SiO_2. Indeed, we have found that anatase titanium dioxide does, in fact, catalyze growth of SiO_2 on its surface.

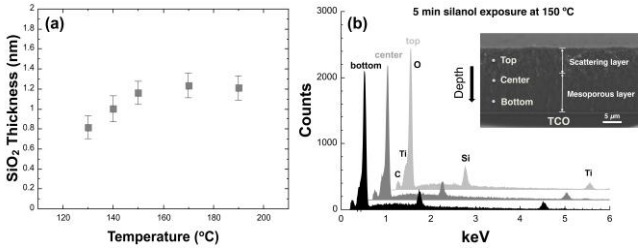

Figure 1. RBS data (a) for the thickness of the SiO_2 layer as a function of deposition temperature and EDS data (b) showing that the silica is deposited uniformly throughout the porous, nanoparticulate TiO_2 electrode.

The SiO_2 coating process was performed in a home-built hot-wall tubular reactor (Scheme 1). Tris(*tert*-butoxy)silanol was used as the precursor for both the silicon and the oxygen. The thickness of SiO_2 deposited on planar witness samples of TiO_2 is plotted as a function of substrate temperature in Figure 1. The reaction temperature was varied from 130 ℃ to 190 ℃, since no SiO_2 film was deposited below 130 ℃. The amount of SiO_2 deposited was measured by the Rutherford Backscattering Spectroscopy (RBS) technique. The thickness of the SiO_2 film was found to increase with temperature from 0.8 nm to about 1.2 nm. These thicknesses represent the self-limited values obtained after initial dosing of about 1 torr of silanol vapor, which was then allowed to react for 5 minutes. Other experiments showed that almost all of this deposition occurs within the first 10 seconds. Energy-dispersive X-ray spectroscopic (EDS) analyses (Figure 1) showed that the SiO_2 is evenly distributed throughout the thousands of TiO_2 nanoparticle (NP) layers constituting the photo-anode. The coverage and thickness of the SiO_2 layer on the TiO_2 NPs were further examined with HRTEM (see Figure 2), which also shows a uniform and conformal SiO_2 layer. The thickness of the SiO_2 layer was ~1 nm and ~3 nm for 140 and 250 ℃, respectively, showing the temperature-dependence of the thickness, consistent with thicknesses determined by RBS.

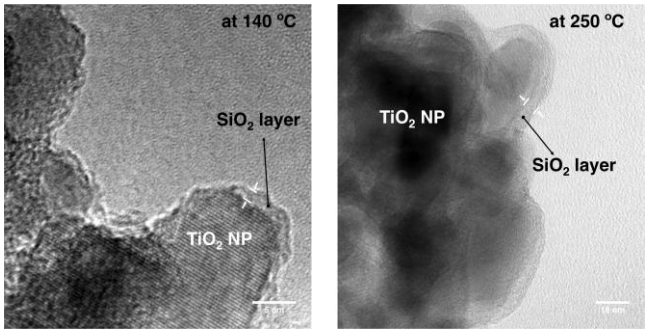

Figure 2. TEM images of TiO_2 nanoparticles coated with SiO_2 at substrate temperatures of 140 °C and at 250 °C.

Although it is not ideal to compare the thickness of SiO_2 on the dye-loaded TiO_2 surface with that on a flat surface, it should be noted that the real thickness of SiO_2 deposited is similar to the vertical dimension of dye molecules as evidenced by the stable oxidation of dyes within TiO_2/SiO_2 films (Figure S1) and the corresponding I–V performance studied below (see Table 1). (Thicker layers might shut-off dye electrochemistry.) In UV-vis spectra of TiO_2/**OrgD**/SiO_2 films, no significant decrease in absorbance is observed after SiO_2 deposition, indicating the sensitizing dye molecules are not affected by the SiO_2 precursor or the thermal stress during SiO_2 deposition (Figure S2 and S3). Given the fact that the sensitized dye molecules are partly surrounded by the SiO_2 layer, resulting in a change of the external dielectric field, the unchanged λ_{max} in the films arises from the low dielectric constant of SiO_2 (ε = ~ 4), which acts as a non-polar medium.

Enshrouding dyes with a glass (silica) coating of precise and uniform thickness substantially improves the photovoltaic performance of the DSC devices. Figure 3 shows action spectra in the form of monochromatic incident photon to current conversion efficiencies (IPCEs) for DSCs based on **OrgD** (electrolyte: 0.6 M DMPImI, 0.05 M iodine, 0.1 M LiI, and 0.5 M *tert*-butylpyridine in acetonitrile). The post-dye treated **OrgD**/$(SiO_2)_x$ (x = SiO_2 deposition temperature ranging from 130 to 170 ℃) cells clearly exhibited an increased response over the entire spectral region, but especially the red region, relative to the non-treated **OrgD** cell. The IPCE of **OrgD**/$(SiO_2)_{130\text{-}170}$ showed plateaus of over 75% from 400 to 590 nm. Significantly higher responses were observed over the wavelength range of 500-700 nm for **OrgD**/$(SiO_2)_{130\text{-}170}$ cells compared to **OrgD** cell. The broadened IPCE of these coated cells suggest superior electron collection capability (greater collection length) versus untreated cells. If we examine IPCE as a function of light harvesting efficiency (LHE) over the wavelength, the results suggest that the coated films have much longer *effective* light infiltration compared to uncoated ones (effective = ability to inject electrons that are subsequently collected as a photocurrent rather than lost to interception by I_3^- or recombination with oxidized dye). As shown in figure S4, if using the LHE of the film at 6-μm-thickness as a standard LHE (thicker film yields absorbance beyond the limit of our instrument), IPCEs of coated electrodes show a shape similar to the LHE line shape expected for a 26-μm-thick electrode (neglecting light scattering and reflectance effects). (See SI for further description.)

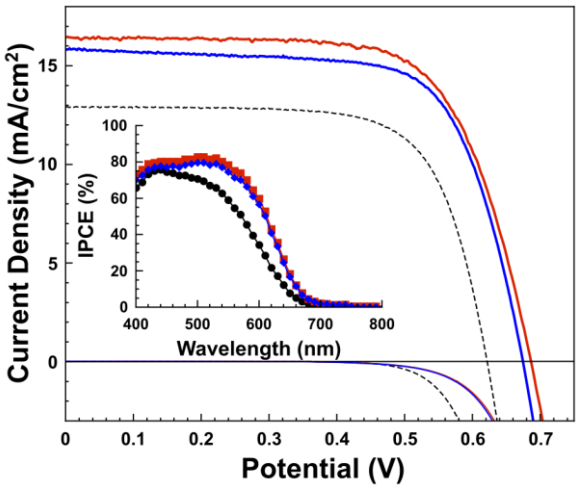

Figure 3. J−V curves, dark currents, and IPCE plots (inset) of **OrgD** (black dash line), **OrgD**/$(SiO_2)_{140}$ (red line), and **OrgD**/$(SiO_2)_{150}$ (blue line).

TABLE 1. Photovoltaic performance of DSCs

Sample	J_{sc} [mA/cm^2]	V_{oc} [V]	FF	η [%]
OrgD	12.93	0.62	0.71	5.67
OrgD/$(SiO_2)_{130}$	14.34	0.66	0.69	6.53
OrgD/$(SiO_2)_{140}$	16.42	0.69	0.68	7.72
OrgD/$(SiO_2)_{150}$	15.83	0.68	0.69	7.41
OrgD/$(SiO_2)_{170}$	15.69	0.67	0.65	6.88
N719	17.66	0.77	0.71	9.61

In contrast, the IPCE from naked electrodes shows a shape similar to the LHE shape for a 10-μm-electrode. From this estimation, we may conclude that the effective length of the coated electrodes is about 2.6 times higher than the uncoated one. The photovoltaic performances of the **OrgD** sensitized cells are listed in Table 1. The optimal condition for the SiO_2 barrier was that produced at 140 ℃ (~1.0 nm by RBS), which resulted in 37% increase in efficiency (η) compared to the reference cell, with the highest η achieved being 7.72%; both the open-circuit photovolatage (V_{oc}) value of 0.69 V and the short-circuit photocurrent (J_{sc}) value of 16.42 mA/cm^2 are larger than for the uncoated control.[17] Under the same conditions, the **OrgD** cell gave J_{sc} = 12.93 mA/cm^2, V_{oc} = 0.62 V, and fill-factor (*ff*) = 0.71, which correspond to η = 5.67%. When the deposition temperature was increased to 150 ℃, the resulting device showed slightly poorer characteristics than the **OrgD**/$(SiO_2)_{140}$ cell. Of particular importance is the 60-70 mV increase in the V_{oc} value of the **OrgD**/$(SiO_2)_{130\text{-}170}$ cell relative to the **OrgD** cell. This result implies that the SiO_2 surrounding the dye results in retardation of interfacial charge recombination losses in the device, as confirmed by the dark current data (Figure 3). Charge lifetimes (τ_e) determined from V_{oc} decay measurements are shown in Figure 4a. The τ_e values are successively shifted to larger values with increase of reaction temperature from 130 to 170 ℃, demonstrating that the electron-recombination process was effectively retarded by the SiO_2 deposition. Specifically, the increase of τ_e by the post-dye SiO_2 layer is saturated with the amount produced at 140 ℃, showing that as little as 1.0 nm of SiO_2 (about 4 monolayers) is sufficient to insulate the TiO_2 surfaces very efficiently. These results are also in good agreement with the V_{oc} results shown in Table 1.

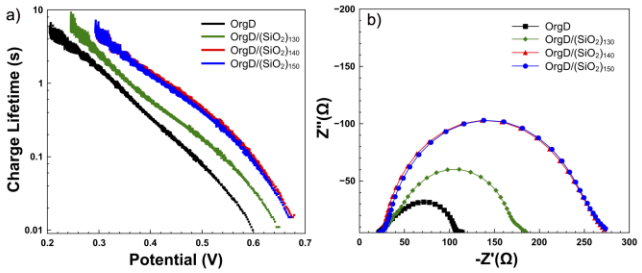

Figure 4. Charge lifetimes from open-circuit photovoltage decays (a) and dark electrochemical impedance spectra (EIS) at 575 mV (b) of **OrgD**, **OrgD**/$(SiO_2)_{130}$, **OrgD**/$(SiO_2)_{140}$, and **OrgD**/$(SiO_2)_{150}$ cells.

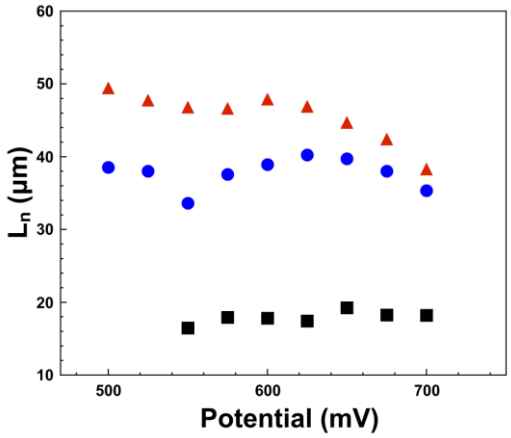

Figure 5. Effective electron diffusion lengths (from dark EIS) for the electrodes coated with **OrgD** (black squares), **OrgD**/$(SiO_2)_{140}$ (red triangles), and **OrgD**/$(SiO_2)_{150}$ (blue circles).

Electrochemical impedance spectroscopy (EIS) was performed under dark conditions (Figure 4b) with the forward bias ranging from −0.5 V to −0.7 V. The semicircular curve obtained in the intermediate-frequency regime shows the dark reaction impedance caused by electron transport from the TiO_2 conduction band to the I_3^- ions in the electrolyte.[18] The radius of the intermediate frequency semicircle showed the increasing order of **OrgD** (72 Ω) < **OrgD**/$(SiO_2)_{130}$ (133 Ω) < **OrgD**/$(SiO_2)_{140}$ (239 Ω) ≤ **OrgD**/$(SiO_2)_{150}$ (241 Ω), which is in agreement with the trends of the V_{oc} and τ_e values. EIS also revealed that the effective length of **OrgD**/$(SiO_2)_{140}$ is roughly 2.5 times greater than **OrgD**, confirming that SiO_2 inhibits the interception of injected electrons by the I_3^- ions in the electrolyte (Figure 5).[19] Figure S5 shows that the untreated and treated cells have a similar capacitance, indicating that the band-edge of the nanoporous TiO_2 network is not affected by the SiO_2 deposition (Figure S5). We envision that this strategy could be even more useful for the bulky outer sphere redox shuttles. Such studies are currently in progress and will be presented elsewhere.

In summary, we have demonstrated that self-aligned, conformal, and self-limiting deposition of SiO_2 on TiO_2 in DSCs is an effective tool for retarding charge recombination, leading to enhanced charge collection and substantially increased overall conversion efficiency. Indeed, the observed 7.72%

efficiency and 16.42 mA/cm^2 J_{sc} values are among the highest yet observed with metal-free dyes (i.e., dyes other than metallo-porphyrins or ruthenium complexes). The SiO_2 layer forms only on the TiO_2 and does not cover the dye molecules. Moreover, this new architecture provides an insulating layer that retards interfacial charge recombination without reducing electron transfer from the dye into the TiO_2 nanoparticles or from the solution to the dye. The optimization of DSCs using this SiO_2 post-dye-treatment as well as the application in different organic dyes is currently being investigated. We believe that the development of highly efficient DSC devices with excellent stabilities is possible through this interfacial engineering.

ASSOCIATED CONTENT

Supporting Information. Detailed description of experimental conditions and results of cyclic voltammetry, UV-Vis, DSC, chemical capacitance experiments. This material is available free of charge via the Internet at http://pubs.acs.org.

AUTHOR INFORMATION

Corresponding Authors

gordon@chemistry.harvard.edu; j-hupp@northwestern.edu

Author Contributions

[‖]These authors contributed equally.

[+]Current address: Centre for Materials Science and Nanotechnology, University of Oslo, Oslo, Norway

ACKNOWLEDGMENTS

Work in the RGG group was performed in part at Harvard University's Center for Nanoscale Systems (CNS), a member of the National Nanotechnology Infrastructure Network (NNIN), which is supported by the National Science Foundation under NSF award no. ECS-0335765. Work at NU was supported as part of the ANSER Center, an Energy Frontier Research Center funded by the U.S. Department of Energy, Office of Science, Office of Basic Energy Sciences under Award Number DE-SC0001059. We also gratefully acknowledge the government of Thailand's Commission on Higher Education for providing partial graduate fellowship support for CP through its program on Strategic Fellowships for Frontier Research Networks.

REFERENCES

(1) (a) O'Regan, B.; Grätzel, M. *Nature* **1991**, *353*, 737. (b) Grätzel, M. *Nature* **2001**, *414*, 338. (c) Wang, P.; Klein, C.; Humphry-Baker, R.; Zakeeruddin, S. M.; Grätzel, M. *J. Am. Chem. Soc*. **2005**, *127*, 808. (d) Robertson, N. *Angew. Chem. Int. Ed.* **2006**, *45*, 2338. (e) Ardo, S.; Meyer, G. J. *Chem. Soc. Rev.*, **2009**, *38*, 115. (f) Hagfeldt, A.; Boschloo, G.; Sun, L.; Kloo, L.; Pettersson, H. *Chem. Rev*. **2010**, *110*, 6595.

(2) (a) Palomares, E.; Clifford, J. N.; Haque, S. A.; Lutz, T.; Durrant, J. R. *J. Am. Chem. Soc.* **2003**, *125*, 475. (b) Clifford, J. N.; Yahioglu, G.; Milgrom, L. R.; Durrant, J. R. *Chem. Commun.* **2002**, 1260.

(3) (a) Koumura, N.; Wang, Z.-S.; Mori, S.; Miyashita, M.; Suzuki, E.; Hara, K. *J. Am. Chem. Soc*. **2006**, *128*, 14256. (b) Choi, H.; Baik, C.; Kang, S. O.; Ko, J.; Kang, M.-S.; Nazeeruddin, M. K.; Grätzel, M. *Angew. Chem. Int. Ed.* **2008**, *47*, 327.

(4) Handa, S.; Haque, S. A.; Durrant, J. R. *Adv. Funct. Mater*. **2007**, *17*, 2878.

(5) (a) Kay, A.; Grätzel, M. *J. Phys. Chem. B* **1993**, *97*, 6272. (b) Schlichthörl, G.; Huang, S. Y.; Sprague, J.; Frank, A. J. *J. Phys. Chem. B*, **1997**, *101*, 8141. (c) Wang, P.; Zakeeruddin, S. M.; Humphry-Baker, R.; Grätzel, M. *Chem. Mater*. **2004**, *16*, 2694.

(6) Choi, H.; Kang, S. O.; Ko, J.; Gao, G.; Kang, H. S.; Kang, M.-S.; Nazeeruddin, M. K.; Grätzel, M. *Angew. Chem. Int. Ed.* **2009**, *48*, 5938.

(7) (a) Feldt, S. M.; Cappel, U. B.; Johansson, E. M. J.; Boschloo, G.; Hagfeldt, A. *J. Phys. Chem. C* **2010**, *114*, 10551. (b) Park, S.-H.; Lim J.; Song, I. Y.; Atmakuri, N.; Song, S.; Kwon, Y. S.; Choi, J. M.; Park, T. *Adv. Energy. Mater*. **2012**, *2*, 219.

(8) (a) Scharrer, M.; Wu, X.; Yamilov, A.; Cao, H.; Chang, R. P. H. *Appl. Phys. Lett.* **2005**, *86*, 151113. (b) Law, M.; Greene, L. E.; Radenovic, A.; Kuykendall, T.; Liphardt, J.; Yang, P. *J. Phys. Chem. B* **2006**, *110*, 22652.

(9) (a) Ritala, M.; Leskelä, M. *Nanotechnology*, **1999**, *10*, 19. (b) Niinistö, L.; Päivasaari, J.; Niinistö, J.; Putkonen, M.; Nieminen, M. *Phys. Stat. Sol.* (a), **2004**, *201*, 1443.

(10) (a) Groner, M. D.; Fabreguette, F. H.; Elam, J. W.; George, S. M. *Chem. Mater*. **2004**, *16*, 639. (b) Hausmann, D. M.; Kim, E.; Becker, J.; Gordon, R. G. *Chem. Mater*. **2002**, *14*, 4350.

(11) (a) Hamann, T. W.; Farha, O. K.; Hupp, J. T. *J. Phys. Chem. C* **2008**, *112*, 19756. (b) Lin, C.; Tsai, F.-Y.; Lee, M.-H.; Lee, C.-H.; Tien, T.-C.; Wang, L.-P.; Tsai, S.-Y. *J. Mater. Chem*. **2009**, *19*, 2999. (c) Antila, L. J.; Heikkilä, M. J.; Aumanen, V.; Kemell, M.; Myllyperkiö, P.; Leskelä, M.; Korppi-Tommola, J. E. I. *J. Phys. Chem. Lett.* **2010**, *1*, 536. (d) Prasittichai, C.; Hupp, J. T., *J. Phys. Chem. Lett.*, **2010**, *1*, 1611.

(12) Hausmann, D.; Becker, J.; Wang, S.; Gordon, R. G. *Science*, **2002**, *298*, 402.

(13) Burton, B. B.; Boleslawski, M. P.; Desombre, A. T.; George, S. M. *Chem. Mater*. **2008**, *20*, 7031.

(14) (a) Gordon, R. G.; Becker, J.; Hausmann, D.; Suh, S. *Chem. Mater*. **2001**, *13*, 2463. (b) Zhong, L. J.; Daniel, W. L.; Zhang, Z. H.; Campbell, S. A.; Gladfelter, W. L. *Chemical Vapor Deposition*, **2006**, *12*, 143.

(15) Zhong, L. J.; Zhang, Z. H.; Campbell, S. A.; Gladfelter, W. L. *J. Mater. Chem.* **2004**, *14*, 3203.

(16) He, W.; Solanki, R.; Conley, J. F.; Ono, Y. *J. Appl. Phys.* **2003**, *94*, 3657.

(17) In contrast, the commonly utilized co-adsorbent, chenodeoxycholic acid (see ref. S1 in SI), yielded no improvement in efficiency, indicating that here it is ineffective in preventing electrolyte interception of injected electrons.

(18) Wang, Q.; Moser, J.-E.; Grätzel, M. *J. Phys. Chem. B* **2005**, *109*, 14945.

(19) We have previously shown that polarizable organic dyes can form weak complexes with I_3^-, thereby enhancing its local (i.e. interfacial) concentration. (Splan, et al. *J. Phys. Chem. B*, **2004**, *108*, 4111.; see also: O'Regan, et al. *J. Am. Chem. Soc*, **2008**, *130*, 2906). If complex formation is diminished or eliminated by dye encapsulation, this could be an additional means of inhibiting dark current.

Single-nanometer-depth silica encapsulation of dyes adsorbed on TiO_2 films effectively slows electrolyte interception of injected electrons, leading to enhanced charge collection and increased overall energy conversion efficiency.

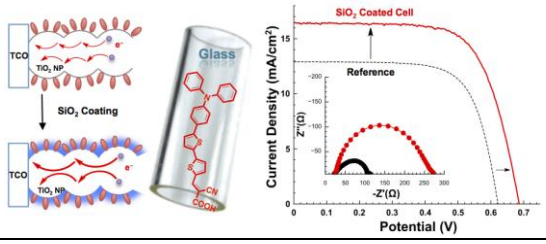
TCO
TiO2 NP
SiO2 Coating
TCO
TiO2 NP
Glass
SiO2 Coated Cell
Reference
Current Density (mA/cm2)
Potential (V)
Z'(Ω)
-Z''(Ω)